

Syndecan-4 Enhances Therapeutic Angiogenesis after Hind Limb Ischemia in Mice with Type 2 Diabetes

Subhamoy Das, Anthony J. Monteforte, Gunjan Singh, Marjan Majid,
Michael B. Sherman, Andrew K. Dunn, and Aaron B. Baker*

Diabetes mellitus affects more than 347 million people worldwide, leading to the death of about 4.6 million people worldwide every year.^[1] Ankle-brachial index screens have determined that the prevalence of peripheral vascular disease (PVD) among diabetics is about 20%–30%.^[2] Of those patients who develop critical limb ischemia, as many as 25% require amputation.^[3] The current clinical standard of care for peripheral ischemia includes physical therapy, pharmacological interventions, endovascular stent placement, and surgical bypass of stenosed arteries.^[4] While these methods provide temporary relief of the patient's symptoms, there are presently no durable, long-term treatment options for patients with severe PVD and accompanying peripheral ischemia. Regenerative strategies for inducing the growth of new blood vessels have the appeal of addressing the fundamental problems of diffuse disease and microvascular involvement that limit current therapies. Many attempts have been made to induce therapeutic angiogenesis; however, clinical trials with the delivery of growth factors,^[5] cytokines,^[6] viral delivery of growth factor genes,^[7] and implantation of bone marrow cells^[8] have only achieved limited success in patients.

One potential reason for these therapeutic failures is that many of the comorbidities that accompany peripheral ischemia, such as diabetes and hyperlipidemia, also create a state in which there is resistance to angiogenic stimulation. If ischemia occurs in a healthy person, compensatory mechanisms induce angiogenesis to restore perfusion. Thus, if a long-term ischemic

condition persists, it implies that endogenous pathways have been interrupted or are insufficient to restore blood flow. We have recently explored the concept of “growth factor resistance” in therapeutic angiogenesis and found that many coreceptors for growth factor signaling are altered in the diabetic disease state.^[9] Among these coreceptors, syndecan-4 is a cell surface, transmembrane protein that is glycosylated with heparan sulfate glycosaminoglycans. Syndecan-4 acts as a coreceptor for fibroblast growth factor-2 (FGF-2) and other growth factors, as well as regulating myriad cellular functions including migration, proliferation, and homeostasis.^[10] Here, we examined whether the delivery of exogenous syndecan-4 could improve angiogenic therapy for ischemia in diabetes. We demonstrate that the delivery of syndecan-4 proteoliposomes (S4PL) markedly improves revascularization in diabetic, hyperlipidemic animals and leads to immune modulation to increase macrophage polarization to the proangiogenic M2 phenotype.

We have previously shown that there is a reduction in protein expression of key growth factor signaling molecules including coreceptors like syndecan-4.^[9] Syndecan-4 plays an important role in the FGF-2 signaling pathway.^[10] Our strategy to circumvent the reduction in syndecan-4 levels was to deliver the missing syndecan-4 coreceptors embedded in a liposomal membrane to enhance the activity of FGF-2 therapy (Figure 1A). We synthesized syndecan-4 proteoliposomes by incorporating the pure syndecan-4 protein in the 400 nm liposomes by serial dilution. We used dynamic light scattering (DLS) to confirm the size of the syndecan-4 proteoliposomes that was found to be around 400 nm (Figure 1F) and cryo-EM to verify the shape and size of the proteoliposomes (Figure 1B,C). For delivery of the compounds in vivo, we decided to use an alginate hydrogel due to its biocompatibility, regulatory approval, and ability to be made injectable. The release kinetics of FGF-2 from the alginate gels with or without S4PL was characterized and we found that S4PL with FGF-2 releases slightly more FGF-2 over 7 d (Figure 1D). We probed the structural features of the alginate gels encapsulating the treatments before being used for the animal studies. Therefore, we lyophilized the alginate gels and imaged them with SEM and found no significant structural differences (Figure 1E). Finally, we performed an in vitro tubule formation assay using human, diabetic endothelial cells and found that syndecan-4 proteoliposomes improved the FGF-2 activity by 24 h of treatment (Figure 1G). Specifically, we found increased numbers of average branch points (Figure 1H) and total tubule length (Figure 1I).

Ischemia is a major contributing factor to the development of nonhealing wounds and diabetic ulcers.^[11] To examine whether syndecan-4 proteoliposomes could significantly overcome

Dr. S. Das, A. J. Monteforte, G. Singh, M. Majid,

Prof. A. K. Dunn, Prof. A. B. Baker

Department of Biomedical Engineering

University of Texas at Austin

Austin, TX, USA

E-mail: abbaker@austin.utexas.edu

Dr. M. B. Sherman

Sealy Center for Structural Biology and Molecular Biophysics

University of Texas Medical Branch at Galveston

Galveston, TX, USA

Prof. A. B. Baker

Institute for Cellular and Molecular Biology

University of Texas at Austin

Austin, TX, USA

Prof. A. B. Baker

Institute for Computational Engineering and Sciences (ICES)

University of Texas at Austin

Austin, TX, USA

Prof. A. B. Baker

Institute for Biomaterials, Drug Delivery and Regenerative Medicine

University of Texas at Austin

Austin, TX, USA



DOI: 10.1002/adhm.201500993

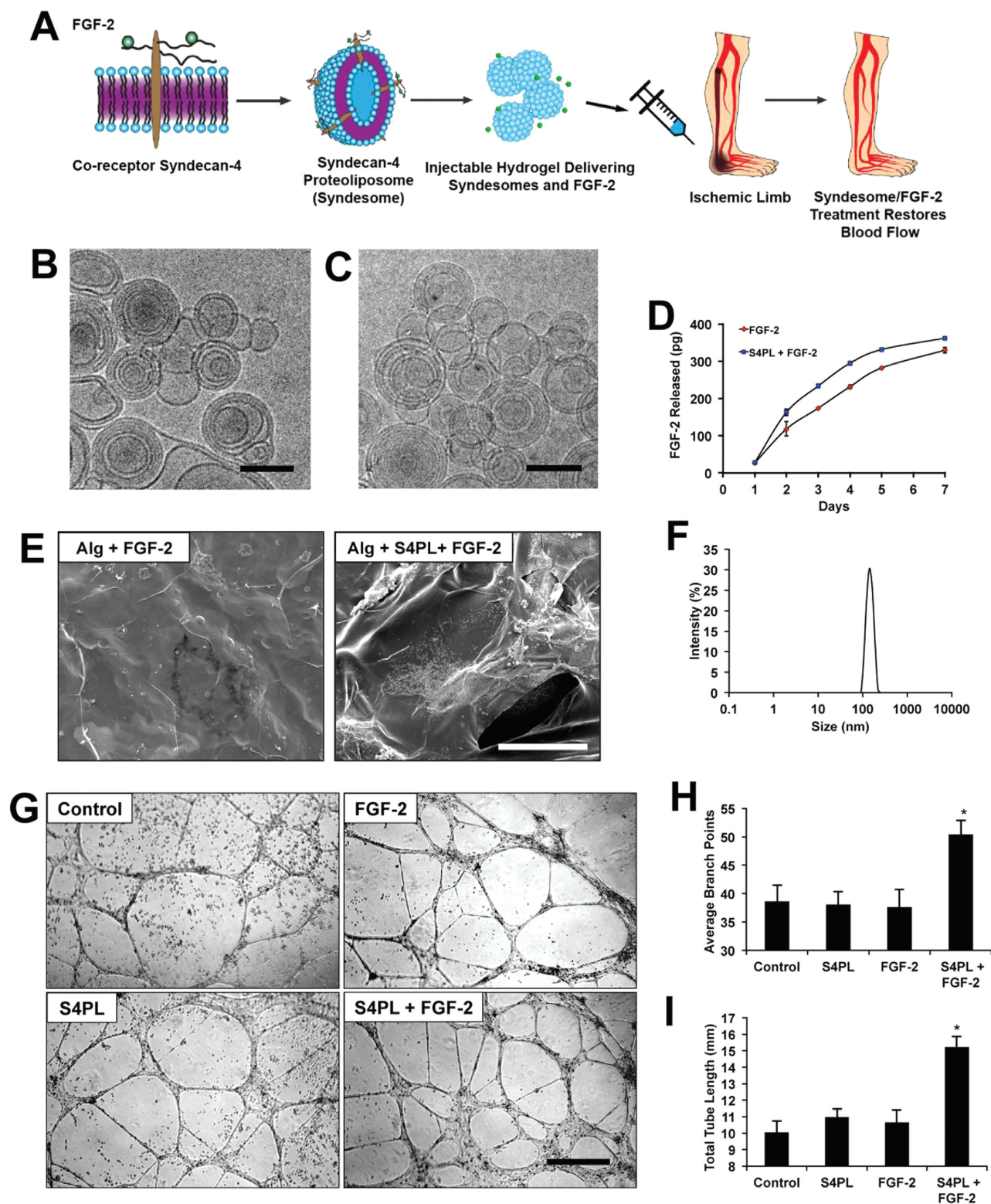


Figure 1. Syndecan-4 proteoliposomes enhance tubule formation in diabetic endothelial cells. A) Graphical representation of the delivery mechanism where the recombinant syndecan-4 embedded in the membrane is codelivered with the FGF-2. B,C) Cryo EM image of the empty liposomes and syndecan-4 proteoliposomes, respectively. Bar = 100 nm. D) Release kinetics of FGF-2 from alginate beads with FGF-2 only (red) or alginate with S4PL+FGF-2 (blue). E) SEM (scanning electron microscopy) image of the lyophilized alginate gel with FGF-2 only or FGF-2 with syndecan-4 proteoliposomes. F) Dynamic light scattering showing the size of the liposomes. G) Tube formation assay on with control, FGF-2, syndecan-4 proteoliposomes (S4PL) and S4PL with FGF-2. H,I) Average number of branch points and total tube length respectively in various treatment groups. *Statistically different from all other treatment groups ($p < 0.05$; $n = 10$).

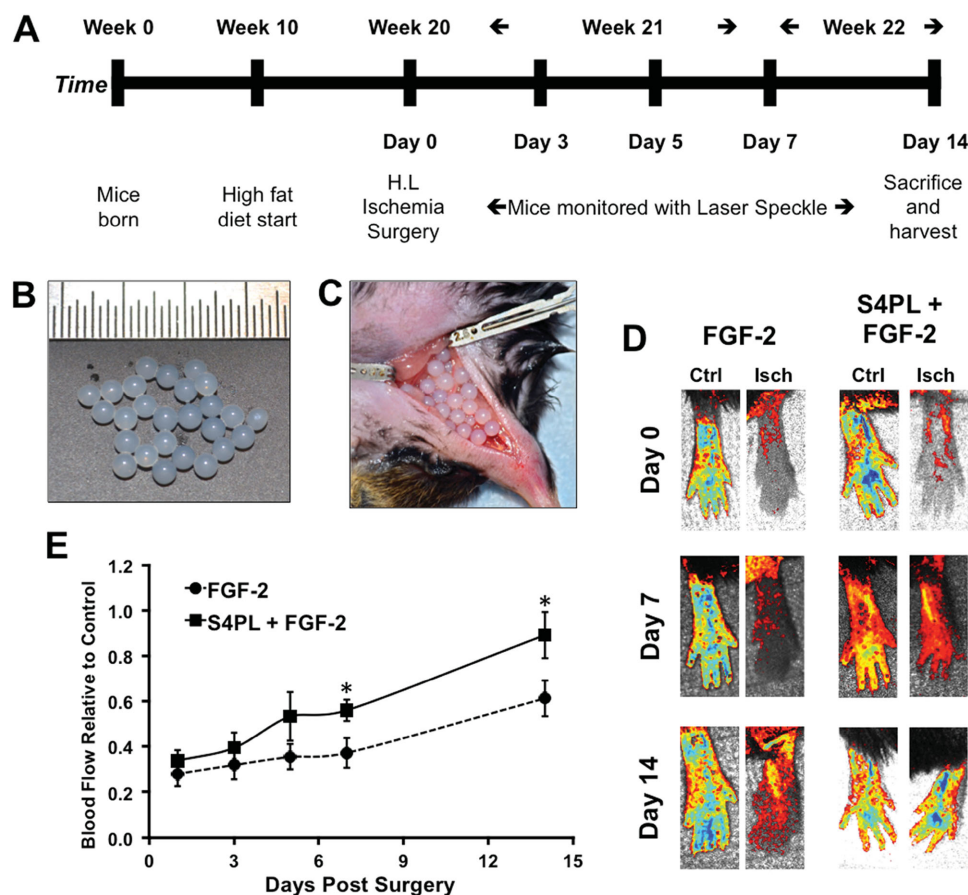


Figure 2. Syndecan-4 proteoliposomes increase blood flow in the ischemic hind limb of ob/ob mice on a high fat diet. A) Study design of the in vivo experiment. B) Treatments were encapsulated in 4% alginate beads. C) The beads were placed in the incision site after the femoral artery ligation. D) Laser speckle contrast imaging of the perfusion of the feet of mice following induction of ischemia. E) Quantitative analysis of perfusion of the ischemic foot normalized to the contralateral control foot. *Statistically different from the FGF-2 only treatment group ($p < 0.05$; $n = 8$).

growth factor resistance in an animal model, we placed ob/ob mice on high fat diet for ten weeks to create a severe diseased state (Figure 2A). We then induced hind limb ischemia in the mice through femoral artery ligation and subsequent removal of a portion of the artery. We implanted alginate beads containing FGF-2 or FGF-2 with syndecan-4 proteoliposomes in the ischemic region (Figure 2B–D). We tracked the recovery in perfusion of the mice feet using laser speckle contrast imaging over 14 d (Figure 2E). A quantitative analysis of the perfusion in the ischemic foot relative to the contralateral control foot revealed a marked increase in the perfusion in the mice treated with syndecan-4 proteoliposomes with FGF-2 (about 86% recovery for the syndecan-4 proteoliposomes/FGF-2 group vs approximately 50% recovery in the FGF-2 group; Figure 2F). After 14 d, the mice were sacrificed and histological analysis of the thigh and calf muscles demonstrated a reduction in the ischemic changes in the muscle fibers for the syndecan-4 treated mice (Figure 3A–D). We performed immunostaining targeted for endothelial cells using a von Willebrand factor antibody and found significantly increased vascularity for both large and small vessels in the thigh and calf muscles (Figure 3E–H). The increase in vascularity in the thigh and calf muscle (Figure 3G,H) was more pronounced compared to

blood perfusion in the feet (Figure 2E). This difference may be due to the presence of immature vessels or due to the fact that the speckle imaging method only measures perfusion in the skin, whereas histological analysis can assess the entire tissue including the muscle.

Macrophages are a key cell type in orchestrating the angiogenic and healing responses in ischemic tissues.^[12] We used immunostaining to examine the expression of the M1 macrophage marker CD86 and the M2 macrophage marker CD163 in the tissue infiltrates surrounding the ischemic injury in the ob/ob mice after 14 d. There was a nonsignificant trend of decreased CD86 in both the thigh and calf muscles of the syndecan- and FGF-2-treated mice in comparison to those treated with FGF-2 alone in both thigh (Figure 4A,C) and calf muscle (Figure 4B,D). In addition, we found an increase in the M2 macrophage marker CD163 in the thigh (Figure 4E,G) and calf muscle (Figure 4F,H) of the mice treated with syndecan-4 proteoliposomes and FGF-2. Notably, there was a significant number of CD163-positive M2 macrophages even at day 14 following ligation, suggesting that active healing was still taking place. These cells would likely aid healing and may be present late into the revascularization process due to the obese ob/ob mouse model used in the studies.

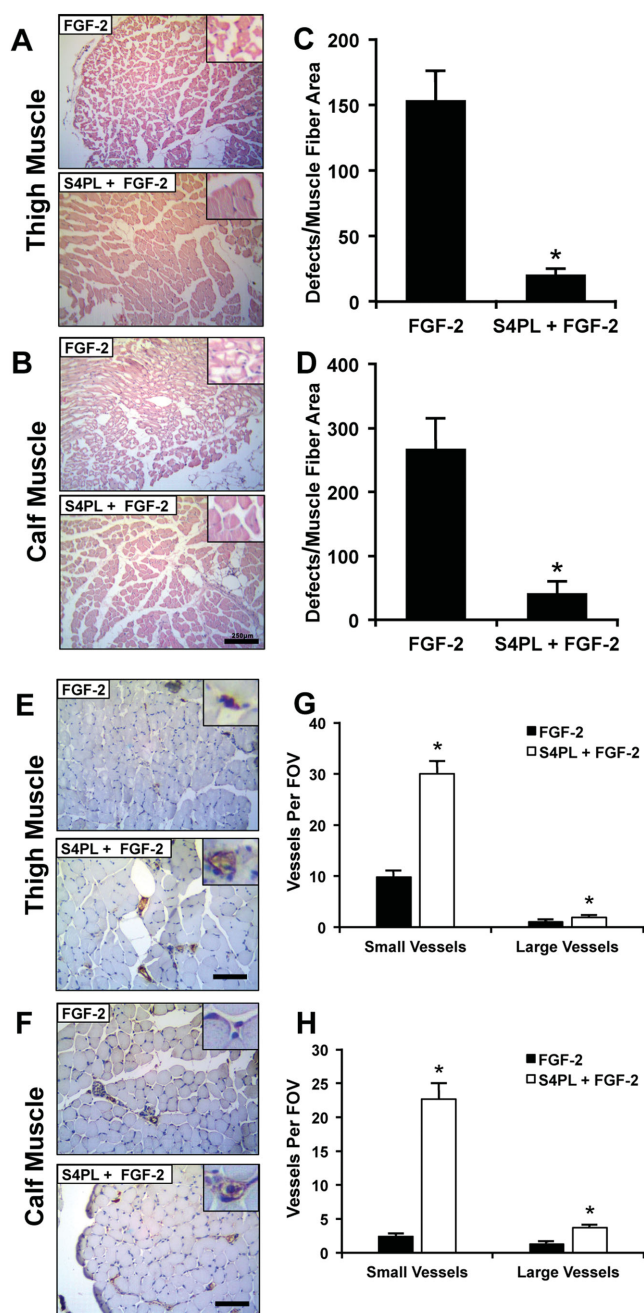


Figure 3. Syndecan-4 proteoliposomes with FGF-2 reduce muscle damage and enhance angiogenesis in the ischemic tissue. A,B) Histological sections from the thigh and calf muscle of the ischemic limbs (Bar = 250 μ m). Inset is magnified threefold. C,D) Quantification of the number of muscle fiber with defects in the thigh and calf muscle of the mice, respectively. E,F) Immunostaining for von Willebrand factor (vWF), which is a marker for endothelial cells in calf muscle sections from the ischemic hind limbs (Bar = 125 μ m). Inset is magnified threefold. G,H) Quantification of the number of vessels per field of view (20 \times magnification image) in thigh and calf muscle sections. *Statistically different from the FGF-2 only treatment group ($p < 0.05$; $n = 8$).

In this study, we have shown that cotherapy with syndecan-4 is effective in enhancing revascularization in the ischemic hind limb of diabetic, obese ob/ob mice. We have previously

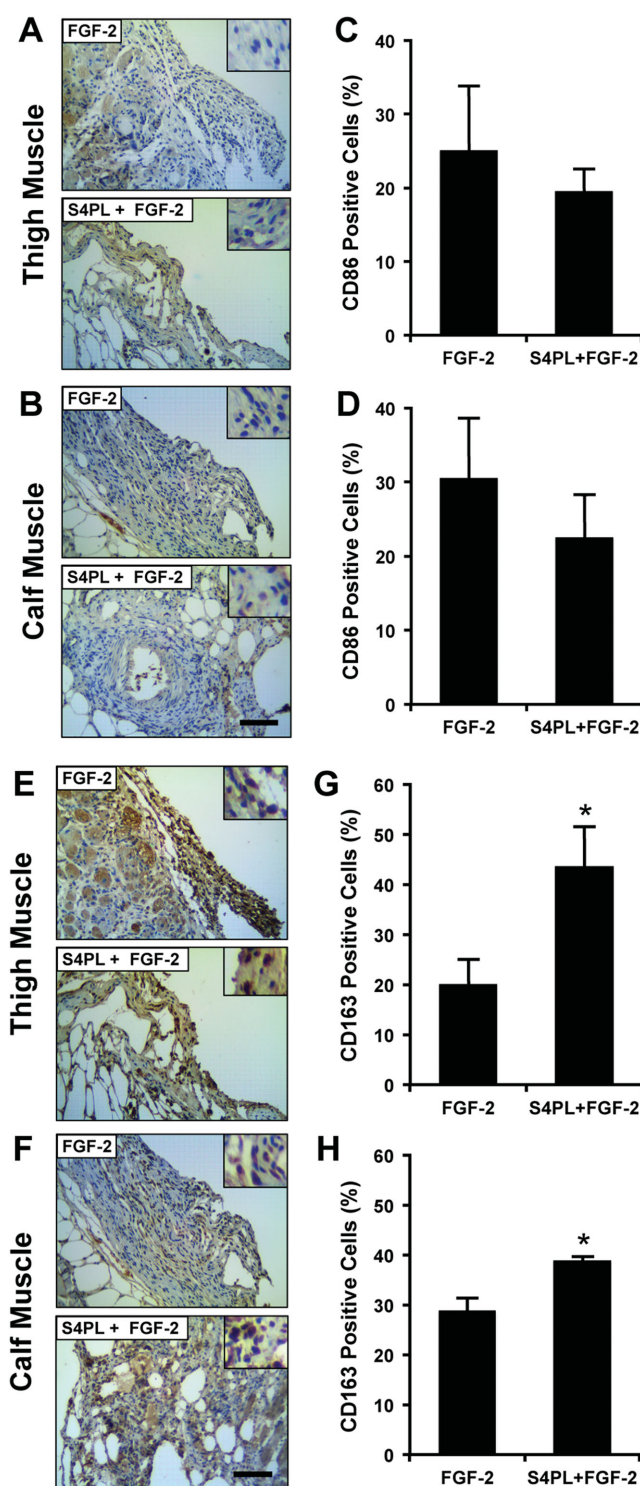


Figure 4. Syndecan-4 and FGF-2-treated limbs have increased staining for M2 macrophage markers. A,B) Thigh and calf muscle sections immunostained for CD86 (M1 macrophage marker). C,D) Quantification of percentage of CD86-positive cells in the thigh and calf muscle. E,F) Immunostaining for CD163 (M2 macrophage marker) in the thigh and calf muscle. G,H) Quantification of percentage of CD163-positive cells in the thigh and calf muscle sections. *Statistically different from FGF-2 only group ($p < 0.05$; $n = 8$). Scale bars = 125 μ m and insets are magnified by threefold.

demonstrated that this mouse model is resistant to growth factor therapy and has reduced expression of syndecan-4.^[9] Here, we examined whether delivery of exogenous syndecan-4 could improve therapeutic angiogenesis in the diabetic disease state. We demonstrate that the syndecan-4 proteoliposomes increase the recovery of perfusion and vessel density following femoral ligation in diabetic, ob/ob mice. This increased angiogenic response was accompanied by an increase in markers for M2-polarized macrophages that have been associated with neovascularization. Together, these results demonstrate that codelivery of syndecan-4 significantly improves the therapeutic potential of FGF-2 in a diabetic model of peripheral ischemia. As syndecan-4 is a major coreceptor in many growth factor signaling pathways, the therapy may have many applications in treating the complications of diabetes including enhancing nonhealing wounds and blood vessel growth in myocardial ischemia.

Experimental Section

Preparation of Syndecan-4 Proteoliposomes: To prepare liposomes, stock solutions (10 mg mL⁻¹) of 1,2-dioleoyl-sn-glycero-3-phosphocholine, 1,2-dioleoyl-sn-glycero-3-phosphoethanolamine, cholesterol, and sphingomyelin were prepared in chloroform. The lipids were mixed in the volumetric ratio 2:1:1 in a round bottom flask and the chloroform was removed on rotatory evaporator attached to a vacuum pump. Liposomes were resuspended in 4-(2-hydroxyethyl)-1-piperazineethanesulfonic acid buffer by vortexing, sonication, and freeze thawing. Finally, an extruding device (Avanti Polar Lipids) with polycarbonate membranes (400 nm) was used to prepare liposomes. A mild detergent, n-octyl- β -D-glucopyranoside (0.1% w/v) was added to both the liposomes and the recombinant syndecan-4. The protein and liposomes were then combined and the detergent was removed by timed serial dilution, dialysis, and treatment with Biobeads (Biorad).

Characterization of Proteoliposomes: The size of the liposomes was measured using DLS using a Zetasizer Nano ZS (Malvern). The instrument was calibrated for size using polystyrene beads (54 nm) before measurement. For imaging with cryo-electron microscopy, the liposomes were plunge-frozen in liquid ethane on carbon holey film grids as previously described (R2x2 Quantifoil; Micro Tools GmbH, Jena, Germany).^[13] The grids were transferred to a cryo-specimen holder (Gatan 626) under liquid nitrogen and put in a microscope (JEOL 2100 LaB6, 200 keV). Grids were maintained at close to liquid nitrogen temperatures during EM session (−172 to −180 °C). Liposomes were imaged at 20 000 \times EM magnification with a CCD camera (UltraScan 895; GATAN, Inc.) using low-dose imaging procedure. Images were acquired with less than 20 electrons per Å² electron dose.

Preparation and Characterization of Alginate Gels: A sodium alginate (Sigma) solution (4% w/v) was prepared in sterile water. The syndecan-4 proteoliposomes and FGF-2 were mixed in the alginate solution as needed. The treatments were loaded in syringes (5 mL) with a 20G needle and extruded drop wise as beads into calcium chloride solution (1.1%) and crosslinked for 1 h at 4 °C. These gels were either used for the release studies or the in vivo hind limb ischemia study.

Tube Formation Assay: Human microvascular endothelial cells isolated from adult skin of type 2 diabetes patients were purchased from Lonza. They were grown in MCDB 131 media with endothelial supplements (Lonza). The cells (passage 2) were grown on growth factor reduced Matrigel (Corning) with various treatments and the plates were imaged over a period of 24 h using an inverted phase contrast microscope (Nikon). The length of the tubule, number of branch points, and the total number of tubules were quantified on Metamorph (Molecular Devices).

Hind Limb Ischemia Model: All animal experiments were performed with the approval of the Institutional Animal Care and Use Committee

of University of Texas at Austin and in accordance with NIH guidelines "Guide for Care and Use of Laboratory Animals" for animal care. All the animal experiments were performed on a diabetic, obese, and hyperlipidemic ob/ob mouse model (B6.Cg-Lep^{ob}/J; Jackson Laboratories). The mice were fed a high fat diet (D12331; Research Diets) for ten weeks before performing the hind limb ischemia studies. To induce ischemia in the hind limb of the mice, an incision was made along the midline of the thigh and the femoral artery was separated from the vein and nerve. The artery was ligated with two 6-0 silk sutures as described in our previous study.^[14] Alginate beads were then applied directly to the region surrounding the femoral artery and the incision site was closed using surgical staples. The feet of the mice were imaged at 1, 3, 5, 7, and 14 d using laser speckle contrast imaging as described below. At day 14, mice were euthanized and the gastrocnemius (calf) and quadriceps (thigh) muscles of both ischemic and contralateral control limbs were harvested. Tissues were snap-frozen in liquid N₂-chilled isopentane and stored at −80 °C until further analysis.

Laser Speckle Contrast Imaging: A custom-made laser speckle contrast imager (LSCI) was used to image the tissue blood flow non-invasively over the course of the study as previously described.^[15] The sample was illuminated with a laser diode (Thor Labs, 785 nm, 50 mW) and the images captured using a Zoom-7000 lens (Navitar) linked to a Bassler CCD camera (Graftek). The blood perfusion in the ischemic limb (hind limb ischemia surgery) was quantified relative of the contralateral control limb. Both limbs were imaged simultaneously using a diffusely focused laser.

Histological Analysis and Immunostaining: The frozen tissues were fixed in paraformaldehyde (4% w/v) and transferred into ethanol (70% w/v). The samples were then paraffin embedded and sectioned using a microtome. Muscle sections were then stained with Hematoxylin and Eosin (H&E) stain for anatomical features.^[9] The samples were also immunostained using antibodies staining for von Willebrand factor (1:1000; DAKO), CD86 (1:250; Bioss), and CD163 (1:100; Bioss). The staining was detected using DAKO Envision kit using a 3,3'-di-amino benzidine (DAB) substrate. The vessel density was quantified by manually measuring the positively stained cells on Metamorph (Molecular Devices). Cells positive for CD86 or CD163 were quantified using the online tool "ImmunoRatio," an automated image analysis software for DAB immunostained images.^[16]

Acknowledgements

The authors gratefully acknowledge support from the American Heart Association (10SDG2630139), the Welch Foundation (F-1836), and the NIH Director's New Innovator Grant (1DP2 OD008716-01) to A.B.B. This work was also supported through the NIH (EB-011556, NS-078791, NS-082518), NSF (CBET-0644638), American Heart Association (14EIA18970041), and the Coulter Foundation grants to A.K.D. A.B.B. and S.D. are guarantors of this work and, as such, had full access to all the data in the study and take responsibility for the integrity of the data and the accuracy of the data analysis. The authors have filed a patent application on the compounds and methods described in this work. The authors acknowledge the Sealy Center for Structural Biology and Molecular Biophysics at the University of Texas Medical Branch at Galveston and the W. M. Keck Foundation for providing research resources.

Received: December 7, 2015

Revised: January 5, 2016

Published online: February 18, 2016

[1] American Diabetes Association, *Diabetes Care* **2013**, 36, 1033.

[2] S. P. Marso, W. R. Hiatt, *J. Am. Coll. Cardiol.* **2006**, 47, 921.

[3] A. M. O'Hare, D. V. Glidden, C. S. Fox, C. Y. Hsu, *Circulation* **2004**, 109, 320.

- [4] M. D. Weinberg, J. F. Lau, K. Rosenfield, J. W. Olin, *Nat. Rev. Cardiol.* **2011**, *8*, 429.
- [5] a) R. J. Lederman, F. O. Mendelsohn, R. D. Anderson, J. F. Saucedo, A. N. Tenaglia, J. B. Hermiller, W. B. Hillegass, K. Rocha-Singh, T. E. Moon, M. J. Whitehouse, B. H. Annex, TRAFFIC Investigators, *Lancet* **2002**, *359*, 2053; b) D. F. Lazarous, E. F. Unger, S. E. Epstein, A. Stine, J. L. Arevalo, E. Y. Chew, A. A. Quyyumi, *J. Am. Coll. Cardiol.* **2000**, *36*, 1239.
- [6] N. van Royen, S. H. Schirmer, B. Atasever, C. Y. Behrens, D. Ubbink, E. E. Buschmann, M. Voskuil, P. Bot, I. Hofer, R. O. Schlingemann, B. J. Biemond, J. G. Tijssen, C. Bode, W. Schaper, J. Oskam, D. A. Legemate, J. J. Piek, I. Buschmann, *Circulation* **2005**, *112*, 1040.
- [7] a) S. Nikol, I. Baumgartner, E. Van Belle, C. Diehm, A. Visona, M. C. Capogrossi, N. Ferreira-Maldent, A. Gallino, M. G. Wyatt, L. D. Wijesinghe, M. Fusari, D. Stephan, J. Emmerich, G. Pompilio, F. Vermassen, E. Pham, V. Grek, M. Coleman, F. Meyer, TALISMAN 201 Investigators, *Mol. Ther.* **2008**, *16*, 972; b) R. Morishita, H. Makino, M. Aoki, N. Hashiya, K. Yamasaki, J. Azuma, Y. Taniyama, Y. Sawa, Y. Kaneda, T. Ogihara, *Arterioscler. Thromb. Vasc. Biol.* **2011**, *31*, 713; c) Y. H. Kusumanto, V. van Weel, N. H. Mulder, A. J. Smit, J. J. van den Dungen, J. M. Hooymans, W. J. Sluiter, R. A. Tio, P. H. Quax, R. O. Gans, R. P. Dullaart, G. A. Hospers, *Hum. Gene Ther.* **2006**, *17*, 683; d) H. Shigematsu, K. Yasuda, T. Iwai, T. Sasajima, S. Ishimaru, Y. Ohashi, T. Yamaguchi, T. Ogihara, R. Morishita, *Gene Ther.* **2010**, *17*, 1152.
- [8] S. Matoba, T. Tatsumi, T. Murohara, T. Imaizumi, Y. Katsuda, M. Ito, Y. Saito, S. Uemura, H. Suzuki, S. Fukumoto, Y. Yamamoto, R. Onodera, S. Teramukai, M. Fukushima, H. Matsubara, *Am. Heart J.* **2008**, *156*, 1010.
- [9] S. Das, G. Singh, A. B. Baker, *Biomaterials* **2014**, *35*, 196.
- [10] A. Elfenbein, M. Simons, *J. Cell Sci.* **2013**, *126*, 3799.
- [11] B. Bruhn-Olszewska, A. Korzon-Burakowska, M. Gabig-Ciminska, P. Olszewski, A. Wegrzyn, J. Jakobkiewicz-Banecka, *Acta Biochim. Pol.* **2012**, *59*, 507.
- [12] T. J. Koh, L. A. DiPietro, *Expert Rev. Mol. Med.* **2011**, *13*, e23.
- [13] M. B. Sherman, R. H. Guenther, F. Tama, T. L. Sit, C. L. Brooks, A. M. Mikhailov, E. V. Orlova, T. S. Baker, S. A. Lommel, *J. Virol.* **2006**, *80*, 10395.
- [14] E. Jang, H. Albadawi, M. T. Watkins, E. R. Edelman, A. B. Baker, *Proc. Natl. Acad. Sci. USA* **2012**, *109*, 1679.
- [15] A. B. Parthasarathy, W. J. Tom, A. Gopal, X. Zhang, A. K. Dunn, *Opt. Express* **2008**, *16*, 1975.
- [16] V. J. Tuominen, S. Ruotoistenmaki, A. Viitanen, M. Jumppanen, J. Isola, *Breast Cancer Res.* **2010**, *12*, R56.